ANALYSIS OF THERMALLY INDUCED DEFECTS IN DC PLASMA SPRAYED THERMAL BARRIERS BY THE USE OF AN ACOUSTIC EMISSION TECHNIQUE.

Joël Voyer, François Gitzhofer and Maher I. Boulos

Plasma Technology Research Center, Department of Chemical Engineering,
Université de Sherbrooke, Sherbrooke, Québec, J1K 2R1, Canada

S. Durham
Pratt & Whitney Canada Inc., Longueuil, Québec, Canada

Abstract

In this study, acoustic emission signals are used to monitor the degradation of plasma sprayed Thermal Barrier Coatings (TBC) under thermal cycling conditions. A classification of the signals based on their energy and their maximum peak frequency is presented.

1. Introduction

Plasma-sprayed thermal barrier coatings are currently used to improve the efficiency of gas turbine engines[1-3]. The coatings used have low thermal conductivity and thermal diffusivity, combined with a good chemical stability at high temperatures[1,4], which helps prevent overheating of the metallic parts of engines. However, coatings applied in engines show unpredictable durability[5]. The major source of failure of TBCs is due to thermally induced delaminations arising from subsurface cracking near the bond coat-ceramic interface[5], leading to spalling and flaking of the coatings[4]. Burner rig tests have been used to study the resistance of the thermal barrier coatings under well controlled conditions[6-8], however, these tests suffer the disadvantage of combining the degradation effects of thermal cycling and oxidation. Since thermal cycling is the primary cause of coatings failure[9], the determination of the effects of the spraying parameters on the resistance of the coatings needs an alternative technique which can discriminate between thermal failure and oxidation failure.

The objective of this study is therefore to develop an advanced material testing technique for the comparative evaluation of TBCs. Such a technique will allow the use of the results of short thermal cycling tests for the prediction of the long term behavior of the coatings under well controlled conditions. The approach is based on the use of acoustic emission techniques coupled with advanced signal processing in

the frequency and amplitude domains of the signals in order to identify and localize any characteristic features that could be correlated with the failure mechanism in the deposit.

2. Experimental setup

The thermal shock test rig developed for this work is based on the use of a high intensity radiative source which can be modulated to control the intensity and the duration of the thermal cycle. Fig. 1 shows an overall schematic of the experimental set-up. Twelve quartz infrared lamps, each with a power rating of 1200 W, are used as the heat source. The lamp mounting is backed by a highly polished, gold coated, water-cooled stainless steel reflector for optimal concentration of the radiated energy onto the specimen surface. A 180 mm external diameter quartz tube is used to isolate the sample from the ambient air in order to allow for the performance of the tests under a controlled inert atmosphere. Fig. 2 shows the details of the experimental set-up.

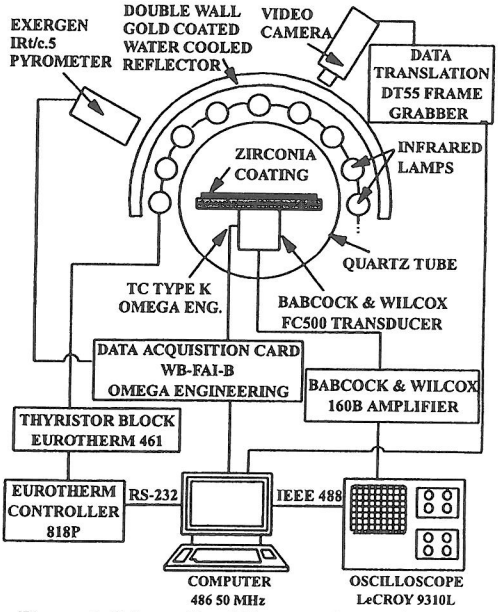

Figure 1 Schematic of the experimental setup

The test sample consists of a metallic alloy substrate (IN 625) which is 370 mm long by 25 mm wide and 750 μm thick, coated with a 125 μm thick plasma sprayed bond coat (NiCoCrAlY) and a 300 μm thick plasma sprayed 20% Yttria Stabilized Zirconia (YSZ) coating over a central 100 mm section of the sample. Throughout the test, a gas purge of argon is used (12 l/min) in order to prevent the oxidation of the bond coat at the interface. During the cooling period of the cycle, a flow of argon directed on the backface of the sample can be optionally used (25 l/min) in order to increase the thermal shock severity.

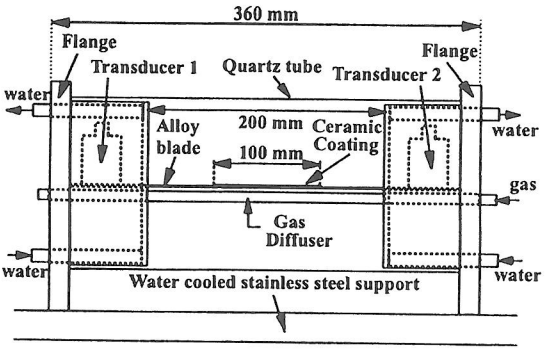

Figure 2 Front view of the setup without reflector

Two ultrasonic transducers are fixed at both ends of the sample so that the sample is used as a wave guide for the acoustic emission signals. The use of two transducers enables the determination of the signals source location. The frequency responses of these transducers are relatively flat between 300 kHz and 2 MHz. Two rubber springs are used to apply pressure on the transducers in order to maintain a perfect contact between the transducers and the sample surface. A coupling medium such as vacuum grease is used for assisting ultrasonics transmission.

3. Signal analysis

A total of 39 parameters are extracted from the acoustic emission signals time and frequency domains, but only three of these are used at the present stage of the investigation to classify the signals. They are :

- Signal energy
- Time of first count over a threshold (mean value + standard deviation)
- Maximum peak frequency.

The signal energy is a direct measure of the magnitude of the acoustic emission source and can characterize different cracking processes[10]. The time measurement provides information on the signal location[10]. Assuming that the signals propagate in the medium at constant speed, the ratio of time taken by the signals to propagate from their source to each of the two transducers located at the extreme ends of the sample is proportional to the ratio of distances traveled:

$$\frac{t_1}{t_2} = \frac{x_1}{x_2} \qquad (1)$$

t_1 ,t_2 = time of detection of the signal by transducer #1 and #2 respectively.
x_1 ,x_2 = distance of signal source from transducer #1 and #2 respectively.

Using this ratio and the total distance between the two transducers, x_1 and x_2 can be calculated, and thus the location of the signals source.

In the frequency domain, differences between power spectra indicate differences in the physical processes giving rise to the acoustic emission signal[11]. General information such as the cycle of emission and the emission temperature of each signal are also stored. With these parameters, a classification of the signals will be made in an attempt to identify the signature of crack initiation and propagation in TBCs.

4. Results and discussion

The thermal cycle used for the tests consists of 4 minutes of heating at full-power of the quartz lamps followed by 4 minutes of cooling with the lamps shut off. As noted earlier, an argon gas jet is used to cool the backface of the sample

during the cooling part of the cycle in order to increase the severity of the thermal shock. A maximum surface temperature of the coating of 1000 °C is attained during the heating period of a typical thermal cycle. The heat flux received by the sample is of the order of 2 MW/m^2 as determined by a simple calculation.

A total of 43 cycles were carried out on a sample of TBC. A total of 46 acoustic emission signals were recorded from the sample (46 signals picked up by each transducer for a total of 92 signals). Fig. 3 shows a typical signal recorded by both transducers in the time domain. Its corresponding frequency components are shown on Fig. 4. In this case, the signal arrives at transducer #1 first. Attenuation

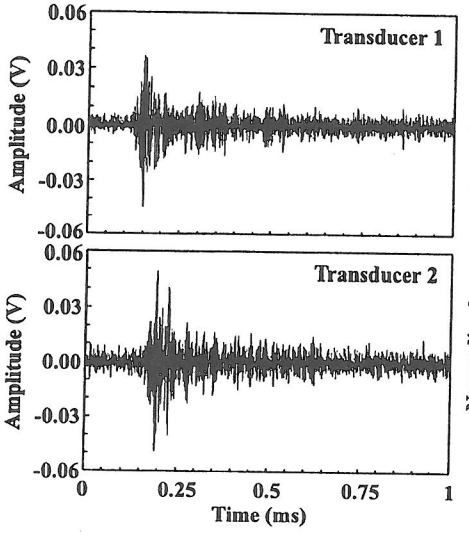

Figure 3 Signals in time domain

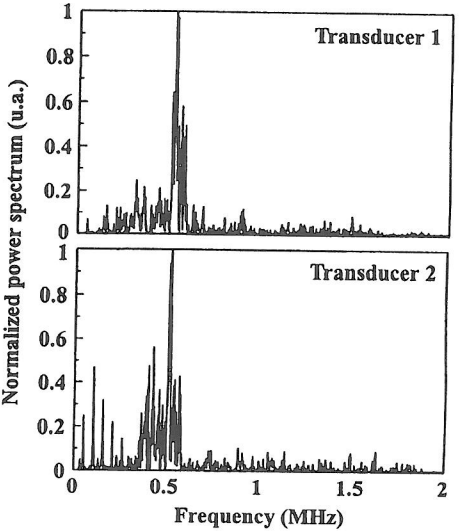

Figure 4 Normalized power spectrums

effects of the propagation medium on the signals can be observed on Fig. 3 by comparing the amplitudes of the signals. In the frequency domain, both signals have a maximum peak frequency around 500 kHz. By comparing the power spectra of the signals displayed in Fig. 4, we see that the signals have essentially the same frequency components. One important feature is that 82 signals out of 92 were emitted during the cooling period of the cycles and the remaining signals were emitted during the heating period. *Enoki et al.*[12] have observed that the acoustic emission signals are mostly emitted during the cooling period in tests similar to ours.

The distribution of signal sources position in the zirconia coating is shown in Fig. 5. The abscissa represents the whole ceramic coating. We clearly see that most of the signals are emitted from two zones on either side of the center of the coating. One of these zones is between 10 mm and 40 mm, and the other between 70 mm and 100 mm. This observation can be explained by the fact that the metallic substrate sample

has undergone plastic deformation as may be seen in Fig. 6. It appears that the two zones described earlier are each centered around the inflection point. Maximum levels of thermal stresses are expected around these two points.

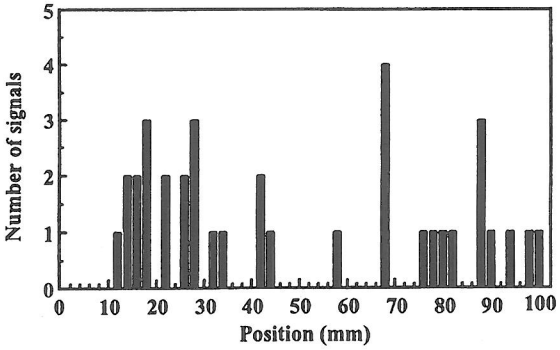

Figure 5 Position distribution of signals

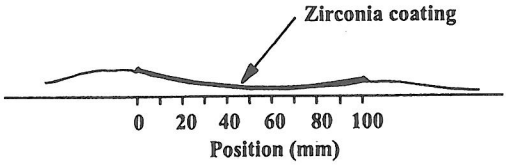

Figure 6 Sample plastic deformation (side view

Fig. 7 shows a plot of the signals energy versus the maximum peak frequency of those same signals. We see that the maximum peak frequency of the three most energetic signals are around 475 kHz for one of them and around 575 kHz for the other two. A means of classification of acoustic emission signals could be based on Fig. 7 since energy level is a measure of the intensity of the degradation mechanism and frequency is a discriminating parameter between different mechanisms. Three distinct groups of signals can be identified from Fig. 7. Those with small energy and small frequency (regime I, with energy < $1x10^{-7}$ V^2s and frequency < 300 kHz), those with small energy and high frequency (regime II, with energy < $2x10^{-7}$ V^2s and frequency > 300 kHz) and finally those with high energy and high frequency (regime III, with energy > $2x10^{-7}$ V^2s and frequency > 300 kHz). Further experiments currently underway, will allow us to go further with such signal analysis procedures with a larger number of emission signals necessary for significant statistical analysis.

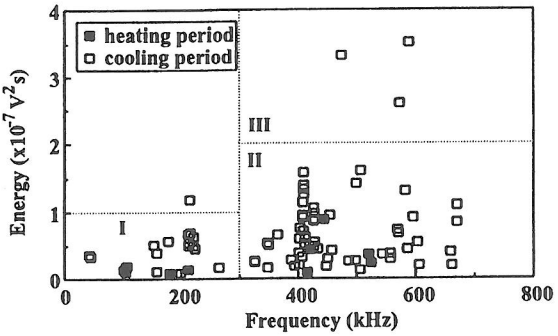

Figure 7 Signals energy versus maximum peak frequency of signals

5. Conclusions

Based on the present study, it can be concluded that the majority of acoustic emission signals are emitted during the cooling period of the thermal cycles and preferentially around each of the two inflection points of the coating. These inflection points are caused by the asymmetric plastic deformation of the metallic substrate sample. When considering the energy and maximum peak frequency of the signals, three distinct regimes can be identified. A group of signals with low energy and low frequency, a group with low energy and high frequency and finally a group with high energy and high frequency. The latter group (high energy and high frequency) consists of three signals that were emitted during the cooling period and at a position of 75 mm which is approximately at one of the inflection point of the substrate. The presence of such high energy and high frequency signals should play a key role in the prediction of long term behavior of the zirconia samples.

Acknowledgment

This project was funded by the Natural Sciences and Engineering Research Council of Canada and Pratt & Whitney Canada through a University-Industry collaboration research program. The financial support by the Ministère de l'Éducation of the Province of Québec through its FCAR-Scholarship to Mr. J.Voyer is gratefully acknowledged.

References

1 Berndt, C.C., J. Eng. for Gas Turbines and Power, **107**, 142-146 (1985).
2 Mori, H., Shiwa, M., Kishi, T., Otsuka, M., Ito, A.,Sugita, Y., Proc. 3rd Japan International SAMPE Symposium, 2330-2334 (1993).
3 Yonushonis, T.M., Stafford, R.J., Ahmed, T., Favro, L.D., Kuo, P.K., Thomas, R.L., Am. Ceram. Soc. Bull., **71**, no.8, 1191- 1202 (1992).
4 Andersson, C.A., Proc. Symposium on the Fracture Mechanics of Ceramics, 450-497 (1973).
5 Dionne, P., Roberge, S., Plasma Spray Process for High Performance Thermal Barrier Coatings, Pratt & Whitney Canada, Technical Report ER-2764 (1193).
6 Ruckle, D.L., Thin Solid Films **73**, 455-461 (1980).
7 Novack, R.C., J. Eng. for Gas Turbine and Power **110**, 617-620 (1988).
8 Watson, J.W., Levine, S.R., Thin Solid Films **119**, 185-193 (1984).
9 Sheffler, K.D., Gupta, D.K., J. Eng. for Gas Turbine and Power **110**, 605-609 (1988).
10 Vahaviolos, S.J., Pollock, A., Lew, N., Chem. Eng. Progr., 60-66 (Jan. 91).
11 Wentzell, P.D., Wade, A.P., Anal. Chem. **61**, 2638-2642 (1989).
12 Enoki, M., Kishi, T., Mäntylä, T., Proc. 3rd Japan International SAMPE Symposium, 2335-2340 (1993).